International Journal of Microwave and Wireless Technologies, 2013, 5(5), 629–636.
doi:10.1017/S1759078713000603

RESEARCH PAPER

Analysis and experimental studies of compact polarization tracking modules for Ku band phased array antennas

WEI SHI[1,2], JUN ZHOU[3,4], ZUPING QIAN[1] AND YA SHEN[4]

Detailed analysis of the polarization tracking modules for Ku band active phased array antennas is presented. The proposed transmitter (14.0–14.5 GHz) and receiver (12.25–12.75 GHz) modules are based on the low temperature co-fired ceramic (LTCC) technique, containing orthogonal dual channels with different phases controlled by phase shifters. The effect of amplitude and phase inconsistency between two channels on polarization tracking performance is analyzed. The validity of the analysis is verified by the measurements of the manufactured prototypes. The measured patterns of the active phased array antenna are given to illustrate the effects of the modules on polarization agility, which may be used for Ku band satellite antennas on mobile terminals.

Keywords: Polarization tracking modules, LTCC, vertical transition, Phased array antenna

Received 28 February 2013; Revised 15 May 2013; first published online 2 July 2013

I. INTRODUCTION

Satellite communication is widely used in military and civilian fields. In order to increase communication capacity, Ku band satellite communication systems usually use orthogonal linear polarizations in the up (14.0–14.5 GHz) and down (12.25–12.75 GHz) links for the frequency reuse. Owing to the mobility of the antenna platforms, such as vehicles, aircrafts, and ships, the antenna platforms will produce yaw, pitch and roll, which will result in change of the beam pointing direction and rotation of polarization orientation of the antenna. For establishing a reliable satellite communication link, in addition to accurate beam pointing of the antenna on mobile terminal, polarization tracking is also required to avoid power loss resulting from polarization mismatch with satellite borne antenna[1, 2].

Phased array antenna may be a suitable solution for Ku band mobile terminal because of its low profile and agile beam. Compared with the conventional mechanically tracking antenna, the phased array antenna steers its main beam pointing toward the satellite continuously by adjusting the phase settings of the modules connected to antenna elements. The variable linear polarization can also be achieved by the phase settings [3]. Consequently, polarization tracking modules based on phase shifters are key components in Ku band polarization tracking phased array antennas.

Nowadays, there is increasing research interest in miniaturization of phased array antennas. Owing to its technical maturity and high dielectric constant, low temperature co-fired ceramic (LTCC) has been widely used to integrate components in a single package with significant reduction of the module volume [4]. Other authors have studied package level integration of LTCC-based antenna for system on package (SOP) applications [5–7]. Various 3D LTCC SOP passive components, such as filters, directional filters, duplexers, and antennas have been demonstrated with excellent performance and high integration potential [8]. Still others have studied an LTCC package fully integrated with 16 antennas and a 60 GHz phased-array transceiver chipset [9]. A Ka band smart antenna array has been developed to demonstrate the interconnection, integration, and package techniques for front end, which contains antenna array and radio frequency (RF) subsystem [10].

This paper proposes Ku band LTCC-based polarization tracking modules for transmitting and receiving phased array antennas. The modules contain two channels connected to the orthogonal feed ports of the antenna element. The orthogonal radiated fields of the antenna elements can be combined to the linear polarization with arbitrary orientation via phase shifters settings. Detailed analysis of the polarization tracking modules is seldom presented in open literatures. The work in this paper studies the effects of the amplitude inconsistency introduced by orthogonal dual channels on polarization tracking accuracy. The initial phase inconsistency introduced by components other than phase shifters in the modules can be compensated for by the phase shifters, thus,

[1]Institute of Communication Engineering, PLA University of Science and Technology, Nanjing, 210016, China. Phone: +86 13851548361
[2]Nanjing Telecommunication Technology Institute, Nanjing, 210007, China
[3]State Key Laboratory of Millimeter Waves, Southeast University, Nanjing, 210096, China
[4]Nanjing Electronic Device Institute, Nanjing, 210016, China
Corresponding author:
W. Shi
Email: sw_ant@sina.com

the phase inconsistency does not degrade the polarization tracking performance.

A 3D LTCC-based coplanar waveguide (CPW)-to-stripline vertical transition building block is developed operating in the Ku band. Based on a hybrid integrated structure using Rogers 4350B soft substrate and hard substrate such as LTCC, we have designed a compact transmitter module operating in the frequency range from 14.0 to 14.5 GHz and a receiver module working in the range from 12.25 to 12.75 GHz. The transmitter and receiver modules have sizes of 12 mm × 11 mm × 3.4 mm and 13 mm × 11 mm × 4 mm respectively. Measured results are given in this paper to verify the correctness of the theory analysis. Based on the modules, we have developed a low profile receive and transmit phased array with a height of 55 and 53.5 mm, respectively. The measured polarization agile patterns are given to illustrate the usefulness of the modules for polarization agility and beam scanning.

II. ANALYSIS

The proposed Ku band transmitter and receiver modules for polarization tracking phased array antennas are shown in Fig. 1, where the orthogonal feed ports of the antenna element are indicated as port H and port V. Arbitrary polarized field can be decomposed into two orthogonal components, such as horizontally and vertically polarized fields illustrated in Fig. 2(a). The antenna element radiates or receives horizontal polarization from port H, and radiates or receives vertical polarization from port V, which is shown in Fig. 2(b). The two output ports of Lange coupler shown in Fig. 1 are connected directly to dual feed ports of the antenna element via microwave cables or connectors. For the receiver module shown in Fig. 1(b), low noise amplifiers (LNAs) are inserted between the Lange coupler and the dual feed ports of the antenna element, so as to decrease the effective noise of the receiver module.

A) Transmitter module

Consider a traveling wave incident on the input port of the power divider. Owing to impedance mismatch and inevitable

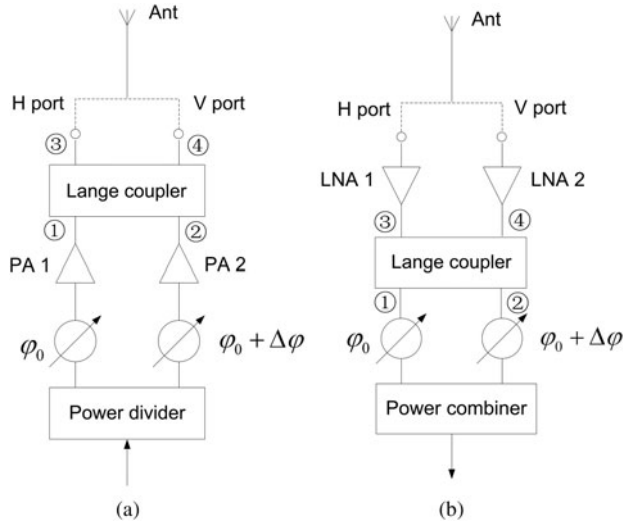

Fig. 1. The schematic circuits of the Ku band polarization tracking modules.

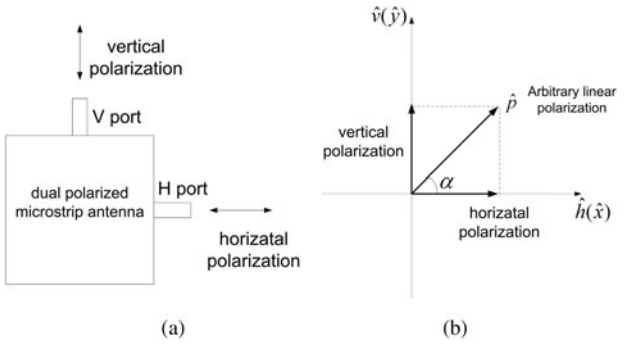

Fig. 2. The generation of arbitrary linear polarization.

inconsistency of the channels, signals arriving at input ports of the Lange coupler are as follows:

$$\text{Port } ①: u_1 = -\frac{j}{\sqrt{2L_0}} a\sqrt{G_0}\Delta_1 \exp(j\varphi_0), \tag{1a}$$

$$\text{Port } ②: u_2 = -\frac{j}{\sqrt{2L_0}} a\sqrt{G_0}\Delta_2 \exp[j(\varphi_0 + \Delta\varphi)]. \tag{1b}$$

Here, L_0 and G_0 indicate the power loss of the transmission and the average gain of the power amplifiers, respectively. Δ_1 and Δ_2 describe the amplitude fluctuation, ideally $\Delta_1 = \Delta_2 = 1$. The differential phase is indicated as $\Delta\varphi$. Consequently, the outputs of the Lange coupler are

$$\text{Port } ③: u_3 = -\frac{a}{2\sqrt{L_0 L_1}}\sqrt{G_0}\Delta_1\Delta_{31}\exp(j\varphi_0) + \frac{j}{2\sqrt{L_0 L_1}}\sqrt{G_0}a\Delta_2\Delta_{32}\exp[j(\varphi_0 + \Delta\varphi)], \tag{2a}$$

$$\text{Port } ④: u_4 = \frac{a}{2\sqrt{L_0 L_1}}\sqrt{G_0}\Delta_1\Delta_{41}\exp(j\varphi_0) - \frac{1}{2\sqrt{L_0 L_1}}\sqrt{G_0}a\Delta_2\Delta_{42}\exp[j(\varphi_0 + \Delta\varphi)]. \tag{2b}$$

Compared with the work given in [3], (2a) and (2b) give the general expressions including inconsistency of the amplitude and phase between two channels. L_1 indicates the power loss of the Lange coupler, and Δ_{ij} is the fluctuation coefficient of transmission from port j to port i, ideally,

$$\Delta_{31} = \Delta_{41} = \Delta_{32} = \Delta_{42} = 1. \tag{3}$$

We assume that the characteristics of the dual channels are consistent, that is $\Delta_1 = \Delta_2 = 1$, the dual outputs of the Lange coupler are obtained from (2a) and (2b) as

$$u_3 = -\frac{a}{2\sqrt{L_0 L_1}}\sqrt{G_0}\sqrt{2[1 + \sin(\Delta\varphi)]}\exp[j(\varphi_0 + \varphi_H)], \tag{4a}$$

https://doi.org/10.1017/S1759078713000603 Published online by Cambridge University Press

Table 1. Relationship between differential phase $\Delta\varphi$ and polarization orientation α based on the assumption of consistency of two channels.

Differential phase $\Delta\varphi$ [°]	Output at port H $\sqrt{1+\sin(\Delta\varphi)}$	Output at port V $\sqrt{1-\sin(\Delta\varphi)}$	Phase difference $\lvert\varphi_H-\varphi_V\rvert$ [°]	Polarization orientation α[°]
0	1	1	0	45
−22.5	0.785	1.175	0	56.2
−4.5	0.541	1.306	0	67.5
−67.5	0.275	1.387	0	78.7
−90	0	1.414	0	90
−112.5	0.275	1.387	180	−78.7
−135	0.541	1.306	180	−67.5
−157.5	0.785	1.175	180	−56.2
−180	1	1	180	−45
−202.5	1.175	0.785	180	−33.7
−225	1.306	0.541	180	−22.4
−247.5	1.387	0.275	0	−11.3
−270	1.414	0	180	0
−292.5	1.387	0.275	0	11.3
−315	1.306	0.541	0	22.4
−337.5	1.175	0.785	0	33.7

$$u_4 = -\frac{a}{2\sqrt{L_0 L_1}}\sqrt{G_0}\sqrt{2[1-\sin(\Delta\varphi)]}\exp[j(\varphi_0+\varphi_V)], \tag{4b}$$

which implies

$$\tan\varphi_H = \frac{\cos(\Delta\varphi)}{1+\sin(\Delta\varphi)}, \tag{5a}$$

$$\tan\varphi_E = \frac{1-\sin(\Delta\varphi)}{\cos(\Delta\varphi)}. \tag{5b}$$

In fact, $\tan\varphi_H = \tan\varphi_E$, that is $|\varphi_H-\varphi_V| = 0,\ \pi$. Equations (4a)–(5b) give two outputs of the Lange coupler neglecting the amplitude inconsistency. It is obvious that the outputs of the Lange coupler are in phase or have opposite phase, in spite of the phase shifter settings. This guarantees linear polarization when the transmitter module is used in combination with the antenna element. It is assumed that the horizontally and vertically polarized field patterns of the antenna element are all isotropic. Then, the combined radiated field of the antenna element can be obtained as

$$u_c = \frac{a}{\sqrt{L_0 L_1}}\sqrt{G_0}\exp[j(\varphi_0+\varphi_H)]\hat{p}, \tag{6a}$$

$$\hat{p} = \frac{\sqrt{2}}{2}\left[\hat{h}\sqrt{1+\sin(\Delta\varphi)} \pm \hat{v}\sqrt{1-\sin(\Delta\varphi)}\right], \tag{6b}$$

where $\hat{p}$ is the unit vector of variable linear polarization. It is concluded from (6a) and (6b) that arbitrary linear polarization can be obtained from differential phase setting $\Delta\varphi$, which is illustrated in Table 1. Beam steering can be obtained from phase setting φ_0 of every antenna element.

If there is amplitude inconsistency between the channels at the input ports of the Lange coupler, neglecting the amplitude inconsistency of the Lange coupler, that is

$$\Delta_1 \neq \Delta_2,\ \Delta_{31} = \Delta_{41} = \Delta_{32} = \Delta_{42} = 1. \tag{7}$$

Substitute (7) into (2a) and (2b),

$$\text{Port ③: } u_3 = -\frac{a}{2\sqrt{L_0 L_1}}\sqrt{G_0}\Delta_1\exp(j\varphi_0) \times\{[-1-\Delta_a\sin(\Delta\varphi)]+j\Delta_a\cos(\Delta\varphi)\}, \tag{8a}$$

$$\text{Port ④: } u_4 = -\frac{a}{2\sqrt{L_0 L_1}}\sqrt{G_0}\Delta_1\exp(j\varphi_0) \times\{-\Delta_a\cos(\Delta\varphi)+j[1-\Delta_a\sin(\Delta\varphi)]\}, \tag{8b}$$

where $\Delta_a = \Delta_2/\Delta_1$, measuring the amplitude inconsistency between two channels. The radiated field of the antenna element can be obtained as

$$u_c = \frac{a}{\sqrt{L_0 L_1}}\sqrt{G_0}\Delta_1\exp(j\varphi_0) \times[\hat{h}\sqrt{1+\Delta_a^2+2\Delta_a\sin(\Delta\varphi)}\exp(j\varphi_H) + \hat{v}\sqrt{1+\Delta_a^2-2\Delta_a\sin(\Delta\varphi)}\exp(j\varphi_V)] \tag{9}$$

Here,

$$\tan\varphi_H = \frac{\Delta_a\cos(\Delta\varphi)}{1+\Delta_a\sin(\Delta\varphi)}, \tag{10a}$$

$$\tan\varphi_E = \frac{1-\Delta_a\sin(\Delta\varphi)}{\Delta_a\cos(\Delta\varphi)}. \tag{10b}$$

Then, $\Delta_a \neq 1$ implies $|\varphi_H-\varphi_V| \neq 0$ and π. Consequently, the amplitude inconsistency results in the

https://doi.org/10.1017/S1759078713000603 Published online by Cambridge University Press

phase difference of two outputs between 0 and π in radian. The ratio of output at port V to output at port H is $|(1+\Delta_a)/(1-\Delta_a)|$, with differential phase $\Delta\varphi$ of two phase shifters set to -90°. Compared with Table 1, elliptical polarization instead of pure vertical polarization at $\Delta\varphi = -90^\circ$ is achieved, which is caused by the amplitude inconsistency of two channels.

B) Receiver module

The receiver module has similar characteristics as transmitter module, since they are reciprocal in theory. The effects of the amplitude inconsistency between two channels on combined polarization are the same as the transmitter module. Phase inconsistency introduced by components other than phase shifters can be compensated for by phase shifters, not affecting the polarization tracking performance.

The transmission response and the equivalent noise are analyzed. We assume that the incident plane wave has the following polarization given in Fig. 2. Referring to Fig. 1(b), the input signals arriving at the input ports of the Lange coupler are:

$$\text{Port } ③: u_3 = a\sqrt{G_{amp}}\cos\alpha, \tag{11a}$$

$$\text{Port } ④: u_4 = a\sqrt{G_{amp}}\sin\alpha. \tag{11b}$$

Assuming that the two channels are consistent, the signal at the output of the receiver module can be obtained as

$$\begin{aligned} u_c = &\frac{a}{2\sqrt{L_T}}\sqrt{G_{amp}}\exp[j(180^\circ - \alpha + \varphi_0)] \\ &+ \frac{a}{2\sqrt{L_T}}\sqrt{G_{amp}}\exp[j(90^\circ + \varphi_0 + \Delta\varphi + \alpha)], \end{aligned} \tag{12}$$

where G_{amp} is the gain of the LNA, and L_T is the average insertion loss in each channel. If the phase factor in (12) satisfies the condition as follows,

$$\Delta\varphi = 90^\circ - 2\alpha, \tag{13}$$

the combined signal has no polarization mismatch loss. In this case, the maximum combined signal is given as

$$u_c = \frac{a}{\sqrt{L_T}}\sqrt{G_{amp}}\exp[j(180^\circ - \alpha + \varphi_0)]. \tag{14}$$

If the input of LNA 1 is fed with the input signal and noise and the other input of LNA 2 is terminated generating a two port network, the noise factor of the receiver module shown in Fig. 1(b) can be measured. An input signal a is assumed at the input port of LNA1. Thus, the output signal u_o can be determined by

$$u_o = \frac{1}{2\sqrt{L_T}}a\sqrt{G_{amp}}\sqrt{2[1+\sin(\Delta\varphi)]}\exp[j(\varphi_0 + \varphi_H)], \tag{15}$$

which leads to

$$S_o = \frac{a^2}{2L_T}G_{amp}[1+\sin(\Delta\varphi)]. \tag{16}$$

If we neglect the LNAs, the effective noise N_{add} of the remaining passive network can be obtained using the thermal dynamic equilibrium method,

$$N_{add} = 2(L_T - 1)T_o. \tag{17}$$

In the measurement, the noise factor of Fig. 1(b) is

$$F_{meas} = \frac{S_i/N_i}{S_o/N_o} = \frac{2}{1+\sin(\Delta\varphi)}\left(F_{amp} + \frac{L_T - 1}{G_{amp}}\right). \tag{18}$$

Here, F_{amp} indicates the noise factor of the LNA. In the measurement with the terminated input port of LNA 2, the two-port measured noise factor varies with phase difference $\Delta\varphi$ between the two channels because of (16). If $\Delta\varphi = 0^\circ$, considering the phase introduced by the Lange coupler, the two channels are not in phase. Therefore, the combined signal power is reduced by half shown in (16), and F_{meas} is approximately twice as much as F_{amp}, which is verified by the measured results shown in the following Fig. 7. If $\Delta\varphi = -90^\circ$, the phase of the Lange coupler contributes to the in-phase combination of the signal, therefore F_{meas} approximates F_{amp}.

III. EXPERIMENTAL RESULTS

A) Performance of the LTCC vertical transition

In microwave modules with LTCC techniques, microwave vertical transmission is used widely to reduce the size of the modules [11–13]. For better bandwidth performance, a vertical transition configuration shown in Fig. 3 is introduced in both transmitter and receiver modules [14], where the LTCC hard substrate and Rogers RO4050B soft substrate for motherboard are used. As shown in Fig. 3, the structure contains vertical transition from CPW on top of the LTCC module to the internal SL (strip-line), and transition from the internal SL to the CPW on the motherboard.

From Fig. 4, it is observed that good agreement can be obtained between the simulated and measured results from 2 to 18 GHz. The measured return loss is better than −16 dB up to 18 GHz, and the insertion loss is less than 1.5 dB. Since the measured result contains insertion loss of about 0.6 dB at 18 GHz introduced by the testboard, simulated and measured results of the insertion loss are a little more different.

B) Measured results of the modules

Based on the schematic circuits shown in Fig. 1 and the vertical transition shown in Fig. 3, we have designed the transmitter and receiver modules for Ku band polarization tracking phased array demonstrator. The developed prototypes are displayed in Fig. 5, where the transmitter module has a size of 12 mm × 11 mm × 3.4 mm, and the receiver has a size of

https://doi.org/10.1017/S1759078713000603 Published online by Cambridge University Press

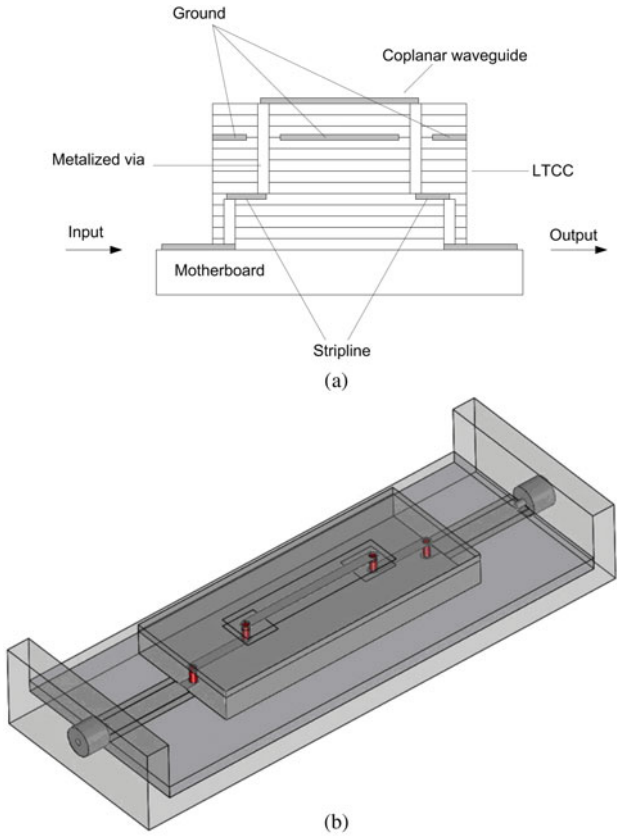

Fig. 3. The vertical transition in the LTCC-based modules.

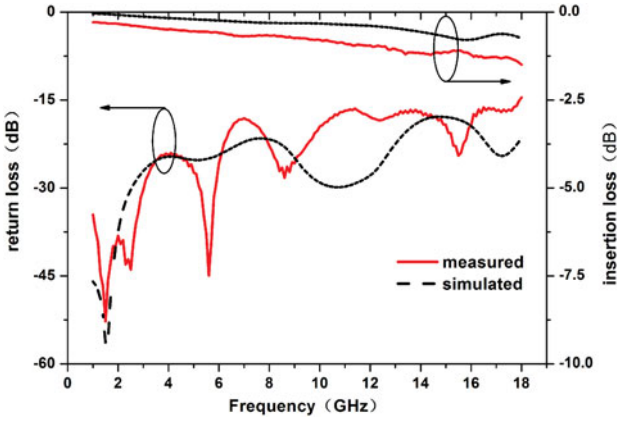

Fig. 4. Return loss and insertion loss of vertical transition.

13 mm × 11 mm × 4 mm. Each module weights about 2.5 g. Various monolithic microwave integrated circuit (MMICs) and control circuits are mounted on top of the LTCC-based modules. The wire bonding technique is used to interconnect microwave transmission lines and MMICs. A lot of logic control lines and power supply lines are buried in the LTCC substrate for high density integration of the modules [15]. In the proposed modules, logic control lines and power supply lines are low frequency circuits, which results in similar design requirements and specifications with the ones of printed circuit board (PCB). Thus, the locations and paths of logic control lines and power supply lines are designed reasonably to meet the requirements of

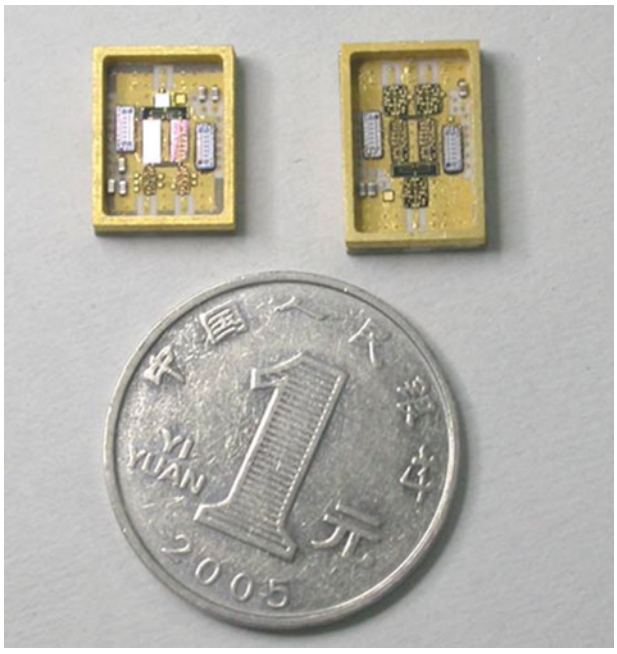

Fig. 5. Photograph of the proposed modules (left: transmitter module, right: receiver module).

electromagnetic compatibility. The RF ports using vertical transition structure shown in Fig. 3(b) and controlling I/O ports are laid on the bottom of the modules. Many metal filled via holes are fabricated for grounding and electromagnetism shielding of layers. A rectangle Kovar frame is attached to the top of the substrate to protect the circuit. A metal cover with 0.1 mm thickness is hermetically soldered on the frame.

When the two phase shifters are set to 0°, the measured gain and output powers of the transmitter module are shown in Fig. 6. The gain of both channels shown in Fig. 1(a) is above 25 dB in the frequency range from 14.0 to14.5 GHz. The output powers of both channels exceed 22 dBm. The amplitude inconsistency of the two channels leads to different gain and different output powers as shown in Fig. 6. The measured gain and noise figure of the receiver module are plotted in Fig. 7, where the receive gain of the two channels shown in Fig. 1(b) is above 29 dB in the frequency range from 12.25 to 12.75 GHz. Similar to the

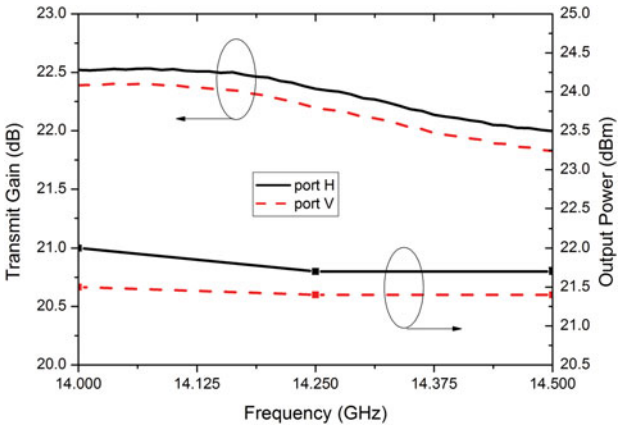

Fig. 6. The measured gain and output powers of the transmitter module ($\Delta\varphi = 0^\circ$).

https://doi.org/10.1017/S1759078713000603 Published online by Cambridge University Press

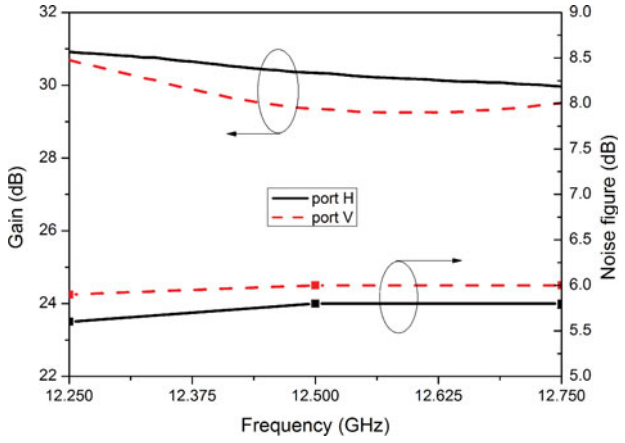

Fig. 7. The measured gain and noise figure of the receiver module ($\Delta\varphi = 0^\circ$).

transmitter module, the inconsistency of the two input channels results in slightly different measured gain at $\Delta\varphi = 0^\circ$. The measured noise figure of each channel is between 5.0 and 6.0 dB. The noise figure of one channel is measured using the noise figure analyzer, with the other channel terminated in 50 Ω load. Thus, the noise from the load increases the measured result, which is expressed explicitly in (18). Then, the measured noise figure of the receiver module will be about twice as much as that of the LNA at $\Delta\varphi = 0^\circ$. In fact, the noise figure of the MMIC used for the LNA is about 2.5 dB, just about one half of the measured results. Thus, the correctness of (18) is verified.

Figures 8 and 9 give the measured gain of two channels for transmitter and receiver module respectively. Owing to reciprocity, it can be seen that the curve shapes of the two figures are basically the same. The following discussion takes the transmitter module as an example. When differential phase $\Delta\varphi$ increases from 0° to −360° with a step of −5.625°, the measured gain of the two channels varied in the range from about −2.5 to 26 dB with different trend, which can be used to control linear polarization of antenna element (Fig. 2). The measured gain of the two ports is almost the same at $\Delta\varphi = 0^\circ$, which contributes to diagonally linear polarization ($\alpha = 45^\circ$). When $\Delta\varphi$ is set as −78.75°, the measured gain of port H and port V is about 2.2 and

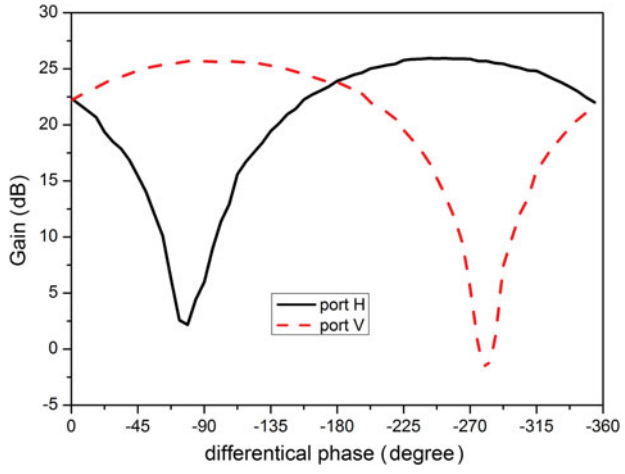

Fig. 8. The measured gain of the transmitter module with $\Delta\varphi$ varying in the range of 360° at 14.25 GHz.

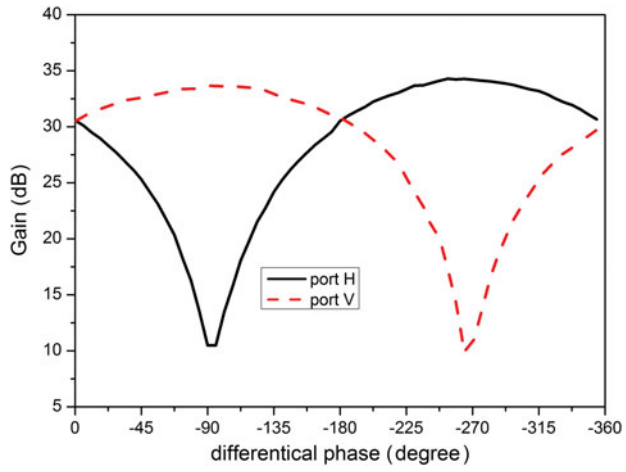

Fig. 9. The measured gain of the receiver module with $\Delta\varphi$ varying in the range of 360° at 12.5 GHz.

25.7 dB respectively, which results in approximately vertical polarization. When $\Delta\varphi$ is set as −281.25°, more output at port H results in approximately horizontal polarization. The phase-controlled variation of the gain given in Fig. 8 produces the arbitrary linear polarization of the antenna element.

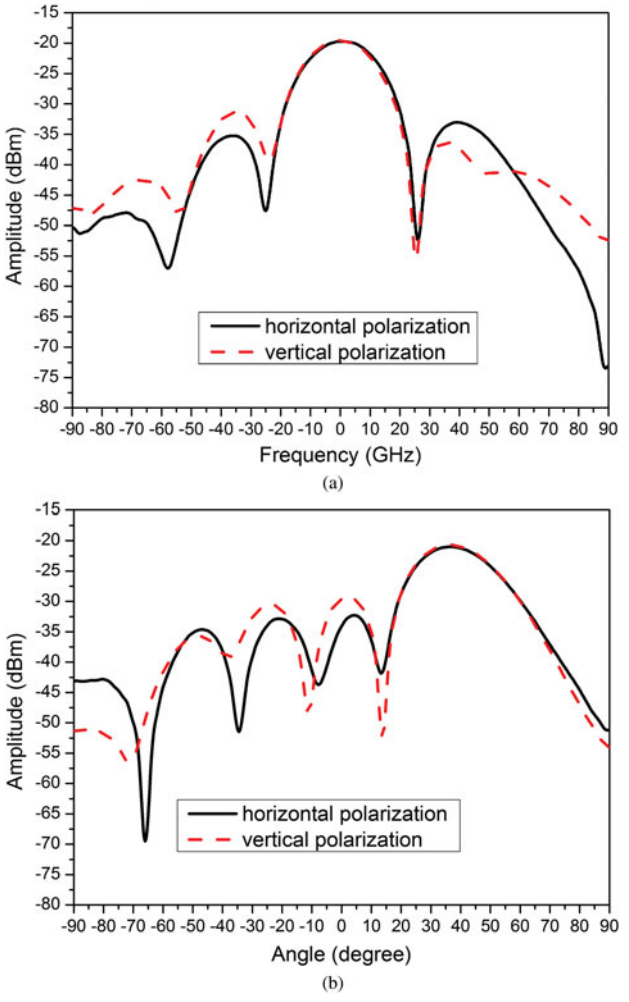

Fig. 10. Measured polarization agile patterns of receive phased array antenna at 12.5 GHz.

https://doi.org/10.1017/S1759078713000603 Published online by Cambridge University Press

Based on the assumption of the consistency of dual channels, the accurate vertical polarization will be obtained at $\Delta\varphi = -90^\circ$, as mentioned in Table 1. However, in the experiment, we have obtained maximum gain of 25.7 dB at port V, and minimum gain of 2.2 dB at port H for $\Delta\varphi = -78.75^\circ$. The deviation of $\Delta\varphi$ from -90° to -78.75° is due to the phase inconsistency of two channels with phase shifters set to 0°. There is small output instead of 0 at port H, which is caused by the amplitude inconsistency of two channels. Thus, pure vertical polarization cannot be achieved. As mentioned in Table 1, horizontal polarization will be achieved with $\Delta\varphi$ set to -270°, since no output exists at port V. However, the experimental results indicate the deviation of $\Delta\varphi$ from -270° to -281.25° due to the phase inconsistency. Amplitude inconsistency contributes to small output at port V. Thus, pure horizontal polarization cannot be obtained. The measured results have verified the correctness of the analysis of inconsistency discussed before. As for the receiver module, same effects of inconsistency exist.

C) Measured patterns of the phased array

Based on the LTCC modules shown in Fig. 5, we have developed two small active polarization tracking phased array demonstrators. The proposed modules result in the low profile receive and transmit phased array antennas with a height of 55 and 53.5 mm, respectively. Both of the phased array demonstrators realized the linear polarization with arbitrary orientation. With the differential phase $\Delta\varphi$ shown in Fig. 1 electronically set to -90° and -270°, the phased array demonstrators have switched the vertical polarization to the horizontal one automatically. The polarization agile patterns at frequencies of 12.5 and 14.25 GHz are illustrated in Figs 10 and 11. While the beam is steered, the polarization agility is realized simultaneously, which can be used to electronically match the polarization of the phased array on mobile terminal to that of the satellite borne antennas.

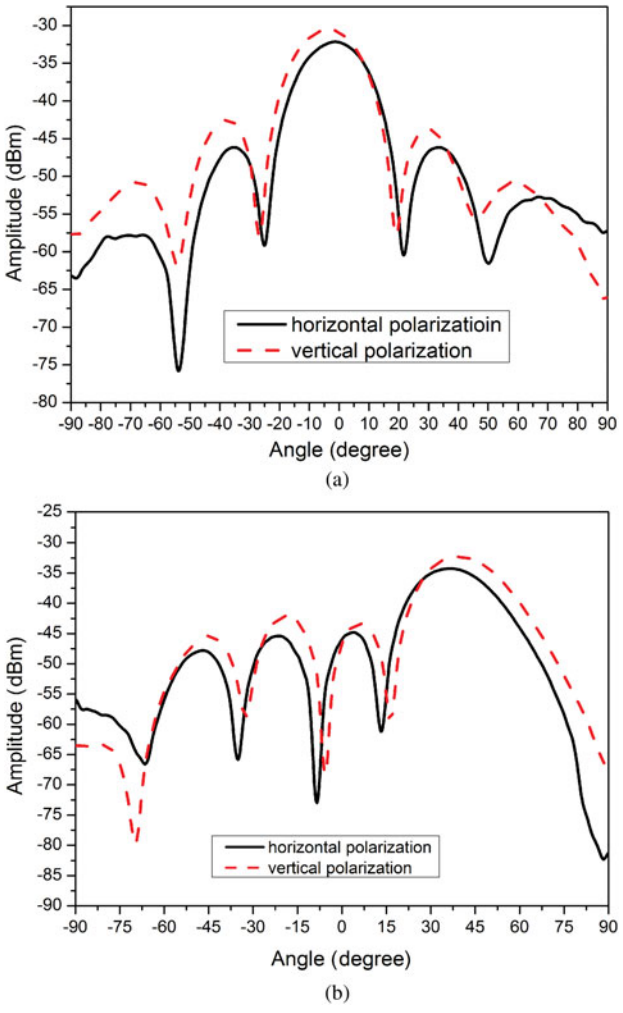

Fig. 11. Measured polarization agile patterns of transmit phased array antenna at 14.25 GHz.

IV. CONCLUSION

This paper has focused on the effects of amplitude and phase inconsistency between two channels on the polarization controlling performance. The effects of the phase inconsistency can be compensated for with the phase shifters, not influencing the accuracy of polarization controlling. However, amplitude inconsistency results in amplitude errors at the outputs of the transmitter module, which affects the polarization controlling accuracy. Large amplitude inconsistency may deteriorate the polarization tracking performance. The receiver module has the same characteristics as the transmitter module. It is impossible to eliminate inconsistency in the orthogonal dual channels because of intrinsic inconsistency introduced by the MMIC components and transmission lines. Therefore, it is crucial to decrease inconsistency in the design process as much as possible. Maybe it is better to use variable attenuators to compensate for amplitude inconsistency, but the complexity and higher cost of the modules will be introduced.

To verify the analysis results, we have manufactured the compact LTCC-based modules for experiment. The measured results are given to validate the correctness of the theory analysis. With the proposed compact modules, low profile receive and transmit active phased arrays with polarization agility are developed for experiment. The measured polarization agile patterns of the phased array demonstrators agreed well, which illustrates the effects of the modules on polarization agility, which can be used for the Ku band phased array for mobile satellite communication. Furthermore, the proposed modules can also be applied in polarization reconfigurable antennas.

REFERENCES

[1] Adler, C.O.; Monk, A.D.; Rasmussen, D.N.; Taylor, M.J.: Two-way airborne broadband communications using phased array antennas, in IEEE Aerospace Conf., Big Sky, USA, March 2003.

[2] Vaccaro, S.; Llorens del Rio, D.; Sánchez, R.T.; Baggen, R.: Low cost phased array for mobile Ku band satellite terminal, in 4th European Conf. on Antennas and Propagation(EuCAP 2010), Barcelona, Spain, April 2010.

[3] van der Bent, G.; de Boer, T.S.; van Dijk, R.; van der Graaf, M.W.; de Hek, A.P.; van Vliet, F.E.: X-band phase-shifting dual-output balanced amplifier MMIC, in 39th European Microwave Conf., Rome, Italy, September 2009.

https://doi.org/10.1017/S1759078713000603 Published online by Cambridge University Press

[4] Kyutae, L. et al.: RF-system-on-package (SOP) for wireless communications. IEEE Microw. Mag., **3** (2002), 88–99.

[5] Wi, S.H. et al.: Package-level integrated LTCC antenna for RF package application. IEEE Trans. Adv. Packag., **2** (2007), 132–141.

[6] Wi, S.H.; Zhang, Y.P.; Kim, H.; Oh, I.Y.; Yook, J.G.: Integration of antenna and feeding network for compact UWB transceiver package. IEEE Trans. Compon. Packag. Manuf. Technol., **1** (2011), 111–118.

[7] Li, R.L. et al.: Design of compact stacked-patch antennas in LTCC multilayer packaging modules for wireless application. IEEE Trans. Adv. Package, **11** (2004), 581–589.

[8] Lee, J.H. et al.: Highly Integrated millimeter-wave passive components using 3-D LTCC system-on-package (SOP) technology. IEEE Trans. Microw. Theory Tech., **6** (2005), 2220–2229.

[9] Kam, D.G.; Liu, D.X.; Natarajan, A.; Reynolds, S.; Chen, H.C.; Floyd, B.A.: LTCC packages with embedded phased-array antennas for 60 GHz communications. IEEE Microw. Wirel. Compon. Lett., **3** (2011), 142–144.

[10] Stark, A. et al.: SANTANA: advanced electronically steerable antennas at Ka-band, in 3rd European conf. on Antennas and Propagation, Berlin, Germany, March 2009.

[11] Bara, T., Jacob, A.F.: Advanced broadband 2nd-level-interconnects for LTCC multi-chip-modules, in German Microwave Conf.(GeMiC2005), Ulm, Germany, April 2005.

[12] Abbosh, A.M.: Ultra wideband vertical microstrip–microstrip transition. IET Microw. Antennas Propag., **10** (2007), 968–972.

[13] Tsai, C.C.; Cheng, Y.S.; Huang, T.Y.; Hsu, Y.A.; Wu, R.B.: Design of microstrip-to-microstrip via transition in multilayered LTCC for frequencies up to 67 GHz. IEEE Trans. Compon. Packag. Technol., **4** (2011), 595–601.

[14] Zhou, J.; Shi, W.; Dou, W.B.; Shen, Y.: High integrated microwave architecture using LTCC-SIP technology in active phased array antenna applications. Frequenz, **6** (2012), 177–182.

[15] Lee, Y.C.; Park, C.S.: A system-in-package (SiP) integration of a 62GHz transmitter for MM-wave communication terminals applications. J. Semicond. Technol.Sci., **3** (2004), 182–188.

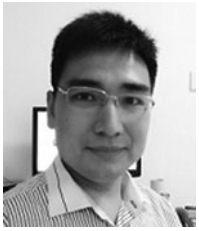

Wei Shi received the MSc degree in Electromagnetic and Microwave Technology from the Institute of Communication Engineering (ICE), PLA University of Science and Technology (PLAUST), Nanjing, China, in 2003. Then, he joined the Nanjing Telecommunication Technology Institute. His main research interests are phased array technique and multiband antenna design. Now, he is working toward a Ph.D. degree in ICE, PLAUST.

Jun Zhou received an MSc degree in Microelectronics and Solid Electronics from China Academy of Electronic and Information Technology, Beijing, China, in 2007. Since then he has joined Nanjing Electronic Device Institute. Now, he is working toward a Ph.D. degree at Southeast University, Nanjing, China. His main research interest is design of high density transceivers.

Zuping Qian received a Ph.D. degree in Electromagnetic and Microwave Technology from Southeast University, Nanjing, China, in 2000. He is currently a Professor with the Institute of Communication Engineering (ICE), PLA University of Science of Technology (PLAUST). His current research interests are in the areas of antenna theory and techniques, array signal processing, and electromagnetic spectrum.

Ya Shen received an MSc degree in Microelectronic and Solid Electronics from Nanjing Electronic Device Institute (NEDI), China, in 1993. He is currently a Professor at NEDI. His research interests include monolithic integrated circuit (MIC) for microwave and millimeter wave applications, and high density transceivers.

https://doi.org/10.1017/S1759078713000603 Published online by Cambridge University Press